Article ID: 1671-3664(2007)02-0135-12 **DOI**:

Intergrain contact density indices for granular mixes — II: Liquefaction resistance

S. Thevanayagam†

Dept. of Civil, Struct., & Env. Eng., State Univ. of New York, Buffalo, NY 14260, USA

Abstract: Whether the presence of non-plastic silt in a granular mix soil impact its liquefaction potential and how to evaluate liquefaction resistance of sand containing different amounts of silt contents are both controversial issues. This paper presents the results of an experimental evaluation to address these issues. Two parameters, namely, equivalent intergranular void ratio $(e_c)_{eq}$ and equivalent interfine void ratio $(e_f)_{eq}$, proposed in a companion paper (Thevanayagam, 2007) as indices of active grain contacts in a granular mix, are used to characterize liquefaction resistance of sands and silty sands. Results indicate that, at the same global void ratio (e), liquefaction resistance of silty sand decreases with an increase in fines content (C_F) up to a threshold value (C_{Fth}). This is due to a reduction in intergrain contact density between the coarse grains. Beyond C_{Fth}, with further addition of fines, the interfine contacts become significant while the inter-coarse grain contacts diminish and coarse grains become dispersed. At the same e, the liquefaction resistance increases and the soil becomes stronger with a further increase in silt content. Beyond a limiting fines content (C_{FL}), the liquefaction resistance is controlled by interfine contacts only. When C_F<C_{Fth}, at the same $(e_c)_{eq}$, the liquefaction resistance of silty sand is comparable to that of the host clean sand at a void ratio equal to $(e_c)_{eq}$. When C_F>C_{Fth}, at the same $(e_f)_{eq}$, the cyclic strength of a sandy silt is comparable to the host silt at a void ratio equal to $(e_f)_{eq}$.

Keywords: Sand; silt; fines; silty sand; liquefaction; cyclic strength

1 Introduction

Sandy deposits that contain a significant amount of fine-grains (silty sands, clayey sands) and/or gravel liquefy during earthquakes and cause lateral spreads (Seed *et al*., 1983; Seed and Harder, 1990; JGS, 1996). Several laboratory and field studies have been conducted to evaluate the effects of increasing silt or gravel content on cyclic strength and liquefaction potential of silty and gravely sands (Chang, 1990; Ishihara, 1993; Seed, 1987; Chameau and Sutterer, 1994; Georgiannou *et al*., 1990, 1991; Vaid, 1994; Koester, 1994; Pitman *et al*., 1994; Singh, 1994; Zlatovic and Ishihara, 1997; Thevanayagam *et al*., 1996; Yamamuro and Lade, 1998; Andrews, 1998; Andrews and Martin, 2000). Laboratory studies show that, at the same (global) void ratio, the cyclic strength of silty sand decreases with an increase in fines content. An example is shown in Fig.1. It indicates the cyclic strength data for five sand-silt mixes (Chang, 1990) prepared by mixing a medium sand (M) with a silt (PI=4) at different silt contents (0%, 5%, 12%, 20%, 45%, and 60% by weight) and tested at an nearly constant global void ratio (e=0.558), initially isotropic consolidated to 104 kPa. At the same cyclic stress ratio, initially, the number of cycles required to cause liquefaction (N_L) decreases with an increase in silt content. Beyond a certain range of silt content, the trend reverses and the strength increases with a further increase in silt content. The transition fines content range is about 20% to 30% for non-plastic fines (Vaid, 1994; Kuerbis *et al*., 1988; Singh, 1994; Koester, 1994; Polito and Martin, 2001). It is less than 20% for clayey (plastic) fines (Georgiannou *et al*., 1991). The conclusions in the literature on whether the presence of fines is beneficial or not to cyclic resistance of soils are contentious. A suitable framework to analyze the influence of fine grains on cyclic strength of such soils is unknown. Similar concerns prevail regarding gravely soils (Evans and Zhou, 1995). Such uncertainties could be resolved if intergrain contact density is considered to be the primary factor that influences liquefaction resistance of soils.

As the void ratio and silt content change, the nature of the microstructure and the relative contribution to the *internal interparticle contact force chain* by different size particles also changes. The stress-strain behavior, liquefaction potential, and fragility of granular mixes are affected by a critical combination of *intergranular and interfine contact* interactions in silty soils. The

Correspondence to: S. Thevanayagam, Dept. of Civil, Struct. and Envir. Eng., 212 Ketter Hall, SUNY at Buffalo, Buffalo, NY 14260, USA
Tel: 716-645-2114 extension 2430
E-mail: theva@eng.buffalo.edu
†Associate Professor

Supported by: National Science Foundation and USGS
Received May 8, 2007; **Accepted** May 22, 2007

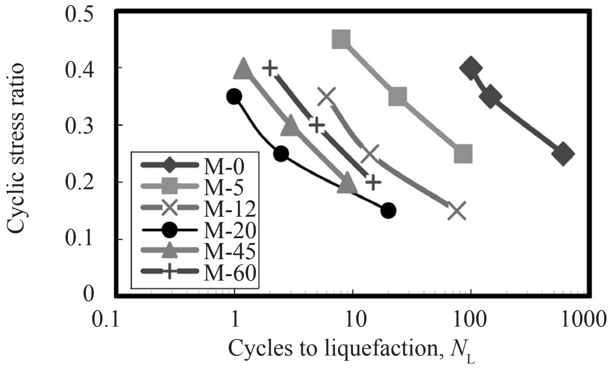

Fig. 1 Influence of silt content on cyclic strength (M-20= Medium sand with 20% silt)

influence of intergrain contact density on liquefaction resistance must be understood and incorporated in order to characterize liquefaction behavior of silty soils. This paper examines the relative contributions of sand and silt grains to the liquefaction resistance of silty soils. Two equivalent intergranular $(e_c)_{eq}$ and interfine $(e_f)_{eq}$ void ratios which have been introduced in a companion paper (Thevanayagam, 2007) as primary indices of intergrain contact density for granular mixes at fine grain contents below and above a certain threshold value (C_{Fth}), respectively, are used to characterize the cyclic strength behavior of granular mixes at any silt content ranging from 0% to 100%.

Table 1 Granular Mix Classification

Case	C_F	e_c	e_f	Roles of coarse-grains and fine-grains
i	$C_F<C_{Fth}$	$e_c<e_{max,HC}$	$e_f>e_{max,HF}$	Fine grains are inactive (or secondary) in the transfer of inter particle forces. They may largely play a role of "filler" of intergranular voids. The mechanical behavior is affected primarily by the coarse grain contacts.
ii	Contact index = $(e_c)_{eq}$	e_c near $e_{max,HS}$		Fine grains support the coarse-grain skeleton that is otherwise unstable. They act as load transfer vehicles between "some" of the coarse-grain particles in the soil-matrix while the remainder of the fines plays a role of "filler" of voids.
iii		$e_c>e_{max,HC}$		Fine grains play an active role of "separator" between a significant number of coarse-grain contacts and therefore begin to dominate the strength characteristics.
iv-2	$C_{Fth}<C_F<C_{FL}$ Contact index = $(e_f)_{eq}$		$e_f<e_{max,HF}$	The fines carry the contact and shear forces while the coarse grains may act as reinforcing elements embedded within the fine grain matrix.
iv-1	$C_F>C_{FL}$	$e_c>>e_{max,HC}$	$e_f<e_{max,HF}$	The fines carry the contact and shear forces while the coarse grains are fully dispersed.

Notes: $e_{max,HC}$, $e_{max,HF}$ = maximum void ratio of the host sand (coarse grains) and host fines (fine grains) media, respectively. They are the limiting void ratios beyond which each soil (clean coarse grained soil, pure fine grained soil) has no appreciable strength. See Eqs.(1)-(6) for expressions for e_c, e_f, C_{Fth}, C_{FL}, $(e_c)_{eq}$ and $(e_f)_{eq}$, respectively.

2 Granular mix classification

It has been recognized that the microstructure of a granular mix, which can be constituted in many different ways with different types of intergrain contacts, significantly affects their mechanical responses. Based on microstructure considerations, a simplified classification system has been developed for granular mixes as shown in Table 1 (Thevanayagam, 2007). Consider a binary granular mix containing particles of size d and D in different proportions. Among many variations, there are three extreme limiting categories of microstructure where (a) primarily the coarse grains are in contact (cases i through iii) with each other, (b) primarily the fine grains are in contact with each other (case iv), or (c) a layered system. Within category (a) there are three subsets: the fines are confined within the void spaces between the coarse grains with little contribution to support the coarse grain skeleton (case i), they partially support the coarse grain skeleton (case ii) or they partially separate the coarse grains (case iii). In category (b), the coarse grains are fully dispersed in the fine grain matrix (case iv).

Case i is possible only if (1) the size, d, of the fine grains is much smaller than the possible minimum pore opening size in the coarse grain skeleton, and (2) the intergranular voids are not completely filled with the fines. Case i is expected to be rare unless the fine grains content is very low. Cases ii and iii are expected to be common. A minor difference between case ii and iii is that, in case iii the fine grains actively participate in the internal force chain by separating the coarse grains and supporting the coarse grain skeleton, whereas they do not in case ii. Case iv is relevant at high fine grains content. At the same void ratio, transition in the microstructure from cases i through iii to case iv can occur naturally with an increase in fine grains content beyond some threshold value (C_{Fth}). At $C_{\mathrm{F}}<C_{\mathrm{Fth}}$ (cases i through iii), the coarse grain contacts play a primary role in the soil's shear response. Fine grains offer a secondary contribution. When $C_{\mathrm{F}}>C_{\mathrm{Fth}}$, the fine grain contacts begin to play a greater role. The coarse grains begin to disperse and offer a secondary reinforcement effect until they are sufficiently separated. This imposes a limiting fines content C_{FL}, above which the fines control the shear behavior (case-iv-2). There exists a transition zone between C_{Fth} and C_{FL} before the behavior of the soil mix is entirely governed by the fine grains (case iv-1).

2.1 Contact density indices

Based on a theoretical analysis of the microstructure of binary mix of particles of size d and D, two sets of first-order and second-order equivalent contact density indices (e_{c}, e_{f}) and (($e_{\mathrm{c}})_{\mathrm{eq}}$, $(e_{\mathrm{f}})_{\mathrm{eq}}$), respectively, have been proposed as possible indices to characterize the mechanical behavior of soils, as shown in Table 1 (Thevanayagam, 2007). The first-order intergranular and interfine void ratios, e_{c} and e_{f} are given by:

$$e_c = \frac{e + c_{\mathrm{f}}}{1 - c_{\mathrm{f}}} \tag{1}$$

$$e_f = \frac{e}{c_{\mathrm{f}}} \tag{2}$$

The e_{c} is also widely known as the sand skeleton void ratio in the literature (Mitchell, 1993; Vaid. 1994; Kuerbis *et al*., 1988; Finn *et al*., 1994; Polito and Martin, 2001). As the fines content increases, the magnitude of e_{c} increases, indicating a decrease in coarse grain contacts; and e_{f} decreases, indicating an increase tendency of interfine grain contacts. Initially, up to a certain C_{Fth}, the magnitude of e_{f} remains very high and the influence of fine grains remains secondary until the e_{f} falls below a threshold value (denoted as $e_{\mathrm{max,HF}}$ in this paper). Up to that point, the shear response of the mix is expected to gradually weaken with an increase in silt content. Once the threshold value of e_{f} is reached, the fine grains are expected to play a primary role. Beyond C_{Fth}, the shear response is expected to strengthen with a further increase in fines content. C_{Fth} is given by (Thevanayagam, 2007):

$$C_{\mathrm{Fth}} \le \frac{100 e_{\mathrm{c}}}{1 + e_{\mathrm{c}} + e_{\mathrm{max,HF}}}\% = \frac{100 e}{e_{\mathrm{max,HF}}}\% \tag{3}$$

where $e_{\mathrm{max,HF}}$ = the maximum void ratio of the pure silt. At $C_{\mathrm{F}}>C_{\mathrm{Fth}}$, the coarse grains become spread apart and the interfine contact friction begins to significantly influence the soil behavior. Unless sufficiently spaced apart, the coarse grains can still (a) engage in friction with fine grains, (b) interfere with the microgeometry of the shear surface, and (c) contribute to redistribution of the normal stresses within the fine grain matrix. This occurs when $C_{\mathrm{Fth}}<C_{\mathrm{F}}<C_{\mathrm{FL}}$. Only beyond $C_{\mathrm{F}}=C_{\mathrm{FL}}$ the soil behavior is governed fully by the interfine friction. The limiting fines content C_{FL} is approximately given by (Thevanayagam, 2007):

$$C_{FL} \ge 100\left[1 - \frac{\pi(1+e)}{6\, s^3}\right]\% = 100\left[\frac{6 s^3 - \pi}{6 s^3 + \pi e_{\mathrm{f}}}\right]\% \ge C_{\mathrm{Fth}}\,; \quad e_f \le e_{\mathrm{max,HF}} \tag{4}$$

where s=1+a/R_{d}, R_{d}=D/d=size disparity ratio, and a=10.

At $C_{\mathrm{F}}<C_{\mathrm{Fth}}$, although one might entirely neglect the secondary effects of fines and use e_{c} as a first-order index of active grain-contacts in a soil mix, due to the influences by the fine grains, the mechanical behavior of such a mix would be stronger than the host coarse grain soil at the same e_{c}. Considering the secondary influence of the fine grains as well, the relevant equivalent intergranular contact index, $(e_{\mathrm{c}})_{\mathrm{eq}}$, has been shown to be of the form (Thevanayagam, 2007):

$$(e_{\mathrm{c}})_{\mathrm{eq}} = \frac{e + (1-b)c_{\mathrm{f}}}{1 - (1-b)c_{\mathrm{f}}}; \qquad 0 < b < 1 \tag{5}$$

where c_{f}=C_{F}/100 and b denotes the portion of the fine grains that contributes to the active intergrain contacts; b=0 would mean that none of the fine grains actively participate in supporting the coarse-grain skeleton; b=1 would mean that all of the fine grains actively participate in supporting the coarse grain skeleton (cases ii and iii). The parameter b depends on grain gradation, packing and size disparity ratio R_{d} (=D/d), and can be determined from gradation characteristics of silty sand (Kanagalinagm and Thevanayagam, 2006).

Similarly, at $C_{\mathrm{Fth}}<C_{\mathrm{F}}<C_{\mathrm{FL}}$, although one may use e_{f} as a first-order approximation for grain contact density in the soil mix, the reinforcement effect by the coarse grains must also be introduced to obtain an equivalent interfine void ratio $(e_{\mathrm{f}})_{\mathrm{eq}}$ as the index of active contacts. For a two size particle system with large size disparity, an approximate expression for $(e_{\mathrm{f}})_{\mathrm{eq}}$ can be derived (Thevanayagam, 20007):

$$(e_{\mathrm{f}})_{\mathrm{eq}} = \frac{e}{c_{\mathrm{f}} + \dfrac{1 - c_{\mathrm{f}}}{R_{\mathrm{d}}^{\mathrm{m}}}} < e_{\mathrm{f}} \tag{6}$$

where 0<m<1 and m = a coefficient that depends on grain characteristics and fine grain packing. Well beyond C_{FL}, the behavior is entirely governed by the fine grains. The interfine void ratio e_{f} may be considered as an index of active contacts. The parameter m can be determined from gradation characteristics of silty sand (Kanagalinagm and Thevanayagam, 2006).

3 Liquefaction resistance and intergrain contact density

This section presents an experimental evaluation of the aforementioned conceptual framework to characterize the liquefaction resistance of granular mixes.

3.1 Experimental program

The experiments in this study involved two sands (OS-F55 and FJ#80) and one non-plastic silt (crushed silica fines Sil-co-Sil #40). Ottawa Silica Sand (OS-F55, US Silica Company, Illinois) was mixed with different amounts of silt at (a) 0%, (b) 15%, (c) 25%, and (d) 60% fines by dry weight. The FJ#80 (The Morie Corporation, Millville) was mixed with 25% of silt. Tests were also conducted on the host sands and 100% silt as well. Table 2 and Fig.2 present the gradation data. Specimens (typically 74 mm diameter and 150-160 mm height) were prepared by placing soils in four layers or eight layers in a triaxial mold using dry air deposition method or moist tamping method. The mold was filled with the soil in layers and each layer was compacted by gentle tamping until reaching a specified target void ratio. Then the specimens were percolated with carbon dioxide for about 5 minutes. After that, de-aired water was allowed to flow from the bottom of the specimen towards the top. This step was omitted for the specimens prepared by the moist tamping method. Then the specimens were set up on a triaxial test apparatus and back-pressure saturated until the B-value ($=\Delta u/\Delta\sigma_c$) was typically greater than 0.95. Following this, the specimens were isotropically consolidated to a constant effective consolidation stress (σ'_c=100 kPa). Stress controlled undrained triaxial cyclic tests were done at a frequency of 0.2 Hz or 1 Hz. The cyclic stress ratio [$R_{CS}=\pm\Delta\sigma_1/(2\sigma'_c)$] was maintained at nearly 0.2. The pore pressure, axial load, and axial deformation were recorded using a built-in data acquisition system. The final void ratio of each specimen was calculated based on the weight of the dry solid grains in the specimen, the net volume of water introduced into the specimen during saturation, and the measured volume change data during consolidation. Experimental details are presented in Thevanayagam *et al*. (2003) and Kanagalingam (2006).

Table 2 Index Properties

Properties	OS-F55 sand-silt					FJ#80 sand-silt	
	OS-00 clean sand	OS-15 silty sand	OS-25 silty sand	OS-60 sandy silt	OS-100 silt	FJ-00 clean sand	FJ-25 silty sand
C_F (%)	0	15	25	60	100	0	25
e_{max} (a)	0.800	0.75	0.86	1.35	2.10	0.935	-
e_{min} (b)	0.608	0.428	0.309	0.413	0.627	-	-
D10 (mm)	0.16	0.018	0.0085	0.0027	0.0015	0.109	0.007
D30 (mm)	0.22	0.19	0.15	0.01	0.006	0.143	0.095
D50 (mm)	0.25	0.235	0.23	0.029	0.01	0.179	0.135
D60 (mm)	0.27	0.245	0.24	0.07	0.015	0.198	0.167
Cu	1.7	13.6	28.2	25.9	10.0	1.8	23.9
Cg	1.1	8.2	11.0	0.5	1.6	0.9	7.7

Notes: (a) = ASTM D4254 (even though this method is recommended only up to 15% fines content), (b) = at optimum moisture content using ASTM D1557.

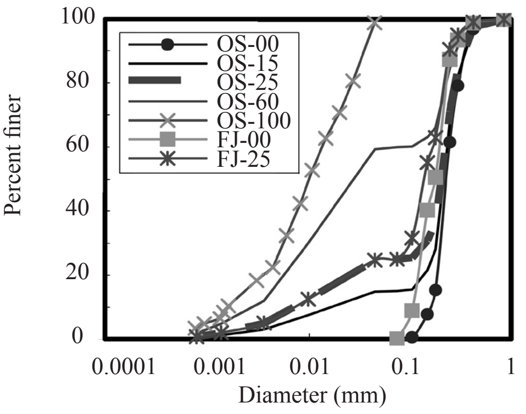

Fig. 2 Grain size distribution of soils

3.2 Liquefaction resistance versus intergrain contact density

3.2.1 Global void ratio

Figures 3(a)-(b) show the data for void ratio versus the number of cycles (N_L) to cause liquefaction at a double amplitude axial strain of ±5% at R_{CS}=0.2 for the two different soil mixes. Fig.3(a) shows the data for OS-F55 sand-silt mix and Fig.3(b) shows the data for FJ#80 sand-silt mixes at silt contents ranging from 0 to 100%. For each soil mix, there is no unique relationship between N_L and global void ratio e for specimens prepared at different silt contents.

At low silt contents less that C_{Fth}, at the same e, N_L decreases with an increase in silt content. This occurs up to threshold silt content of about 25%. At silt contents beyond 25%, the trend reverses and N_L increases with further increase in silt content. If the data at the same N_L is analyzed, the global void ratio required to resist liquefaction decreases with an increase in silt content up to about 25%. The e required to resist liquefaction increases with further increase in silt content beyond 25%. The reason for the lack of a unique relationship between e and N_L is that the microstructure, intergrain contact density and internal contact force chain network within the soil matrix changes with the addition of fines even if the void ratio is kept the same. The liquefaction resistance of the soil changes due to the changes in contact density with addition of fines at the same void ratio. This effect could be better captured if the same data is analyzed using either the first-order or second-order contact density indices e_c and e_f or the second-order indices $(e_c)_{eq}$ and $(e_f)_{eq}$.

In order to evaluate the effect of intergranular contact density on liquefaction resistance, the same data shown in Figs.3(a) and (b) were split into two portions, one for $C_F<C_{Fth}$ and the other for $C_F>C_{Fth}$. The data were first plotted against the first-order contact density indices e_c and e_f, respectively, for OS-F55 (Figs.4(a) and (b)) and for FJ#80 (Fig. 5). Then the same data were also plotted against second-order contact density indices $(e_c)_{eq}$ and $(e_f)_{eq}$, respectively, in Figs. 6 and 7.

3.2.2 First-order indices e_c and e_f

When the data for $C_F<C_{Fth}$ is compared at the same e_c, silty sand still shows higher liquefaction resistance than the host sand (Figs.4(a) and 5). When the data for $C_F>C_{Fth}$ is compared at the same e_f, sandy silt still shows higher liquefaction resistance than the pure silt (Fig.4(b)). The reason for this is that although the first-order indices e_c and e_f are better able to represent the contact density than the global void ratio, they do not fully represent the intergranular contact density of a mix. When calculating the e_c, it is inherently assumed that the silt particles do not contribute to the contacts between the coarser grains. However, a portion of the silt acts as a bridging component between the coarse grains and thus contributes to the strength of the soil. Secondly, the silt particles that lie within the voids between the coarse grains inhibit collapse of the coarse grain skeleton and hence affect the cyclic strength of the soil mix. Similarly,

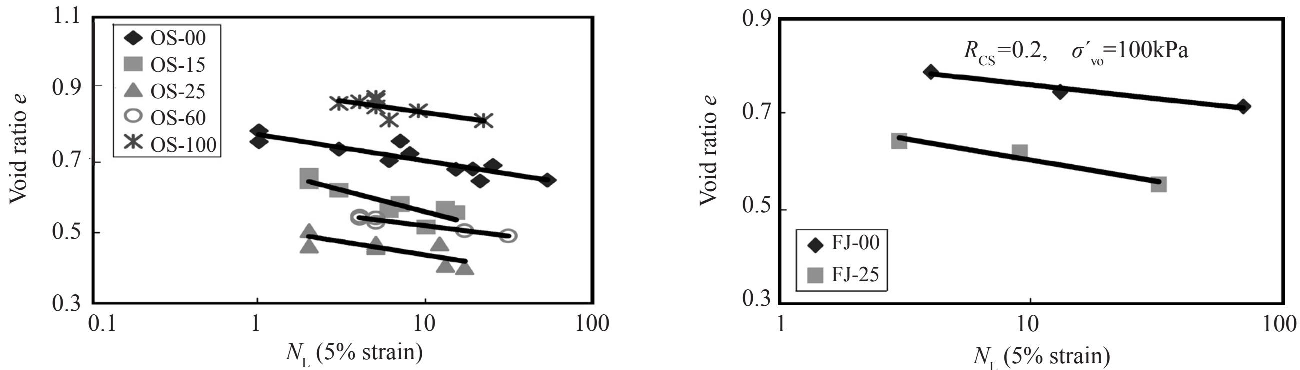

(a) OS-F55 sand-silt mix (b) FJ#80 sand-silt mix

Fig. 3 No. of cycles to liquefaction – N_L vs. e

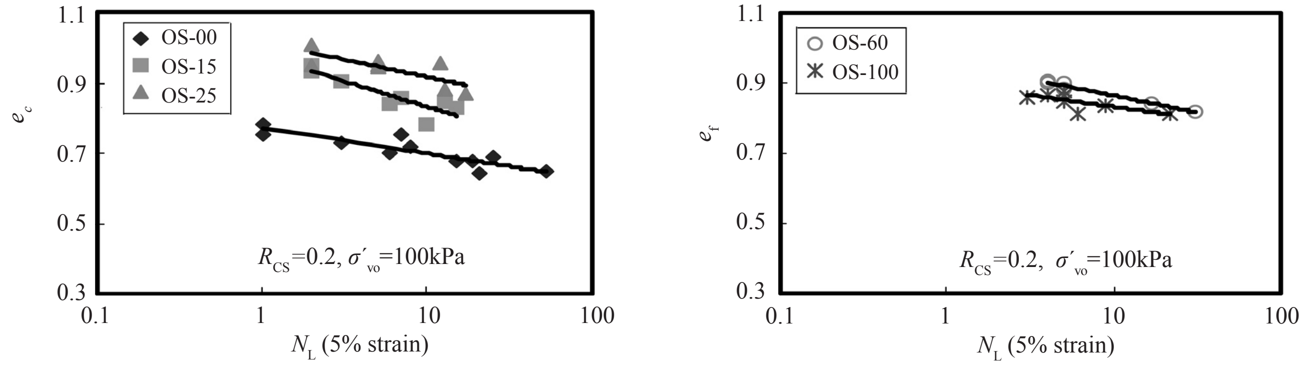

(a) $C_F \le C_{Fth}$ (b) $C_F > C_{Fth}$

Fig. 4 N_L vs. e_c and e_f - OS-F55 sand-silt mix

when calculating the e_f, the effect of coarse grains is completely neglected. However, the dispersed coarse grains indeed provide a reinforcement effect between the fine grains and therefore affect the cyclic strength of the soil. A better correlation is expected in each case if the contributions by the fine and coarse grains are accounted for in the analysis.

3.2.3 Second-order indices $(e_c)_{eq}$ and $(e_f)_{eq}$

Figures 6(a)-(b) show the data for soils containing silt content up to C_{Fth} plotted against $(e_c)_{eq}$ for OS-F55 and FJ#80, respectively. The data in each case fall in a narrow band close to the respective host sands. For each sand there is a strong correlation between liquefaction resistance and $(e_c)_{eq}$ The magnitudes of b used to calculate the relevant $(e_c)_{eq}$ were 0.35 and 0.65 for OS#55 and FJ#80, respectively. The magnitude of b depends on grain shape characteristics, packing, and gradation (Thevanayagam *et al*., 2003; Kanagalingam and Thevanayagam, 2006; Ni *et al*., 2004).

Figure 7 shows the liquefaction resistance versus $(e_f)_{eq}$ data for the sand-silt mixes at silt content beyond C_{Fth} ($C_F > C_{Fth}$) for OS-F55 sand-silt mix. The magnitude of m used to calculate the $(e_f)_{eq}$ for this soil mix was 0.65. The data for the pure silt and sandy silt containing 60%

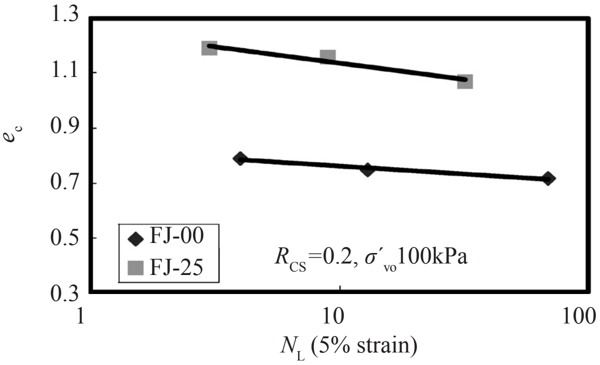

Fig. 5 N_L **vs.** e_c**: FJ#80 sand-silt mix**

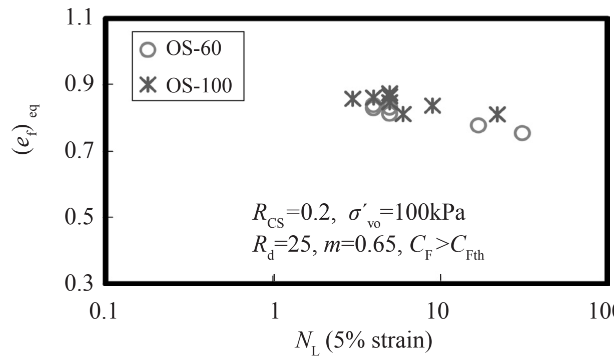

Fig. 7 N_L **vs.** $(e_f)_{eq}$ **for** $C_F>C_{Fth}$

fines merge together when the reinforcement effect by the coarse grains is taken into account.

These observations indicate that the cyclic strength of sand-silt mixes can be better characterized using the equivalent intergranular void ratios $(e_c)_{eq}$ and $(e_f)_{eq}$.

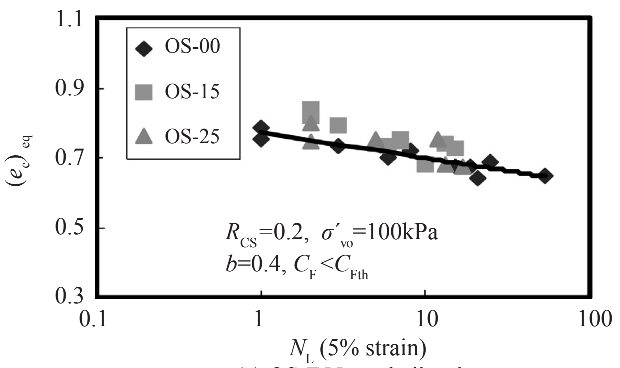

(a) OS-F55 sand-silt mix

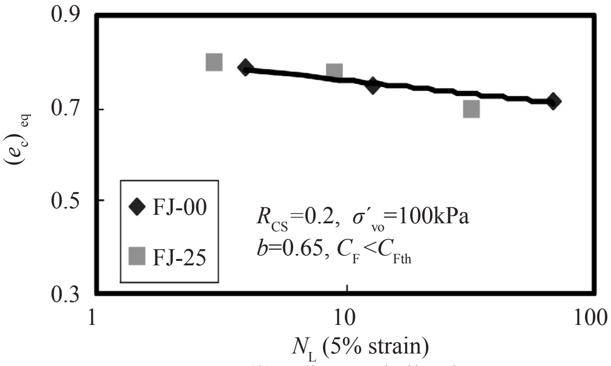

(*b*) FJ#80 sand-silt mix

Fig. 6 N_L **vs.** $(e_c)_{eq}$ **for** $C_F<C_{Fth}$

3.3 Energy to cause liquefaction versus intergrain contact density

Recently, the energy required to cause liquefaction has been introduced as another means to evaluate liquefaction potential of granular soils (Nemat-Nasser and Shokooh, 1979; Davis and Berrill, 1982, 1998a, 1998b; Berrill and Davis, 1985; Law *et al*., 1990; Figueroa *et al*., 1994; Liang *et al*., 1995; Trifunac, 1995; Kayen and Mitchell, 1997; Todorovska and Trifunac, 1999; Desai, 2000). There are a few advantages in using the energy method as it reduces the errors introduced in the determination of the number of cycles to cause liquefaction in cases where a non-uniform cyclic stress history is involved.

The same data shown in Figs.3(a) and (b) were analyzed in terms of the energy required to cause liquefaction, at a double amplitude strain level of 5%, as well. The energy dissipated per unit volume of the soil was calculated using

$$E_L = \sum_{i=1}^{n-1} \frac{1}{2}(\tau_i + \tau_{i+1})(\gamma_{i+1} - \gamma_i) \tag{7}$$

where τ = shear stress; γ = shear strain; n = number of points recorded up to the specific strain levels. The data were first plotted against global void ratio e (Figs.8(a) and (b) for all silt contents, secondly against e_c (Figs.9(a) and (b) for $C_F<C_{Fth}$ and e_f (Fig.9c) for $C_F>C_{Fth}$, respectively, and finally against the second-order contact density indices $(e_c)_{eq}$ (Figs.10(a)-(b) for $C_F<C_{Fth}$ and $(e_f)_{eq}$ (Fig.10(c)), for $C_F>C_{Fth}$, respectively. Similar observations as reported before with reference to Figs. 3 through 7 are found in Figs.8 and 9.

3.3.1 Global void ratio

At the same global void ratio, the energy required to cause liquefaction decreases with an increase in silt content up to C_{Fth}. At silt content beyond C_{Fth}, the trend reverses and the energy required to cause liquefaction increases with further increase in silt content (Fig.8). If the data are analyzed at the same energy required to cause liquefaction E_L, the global void ratio required to resist liquefaction decreases with an increase in silt

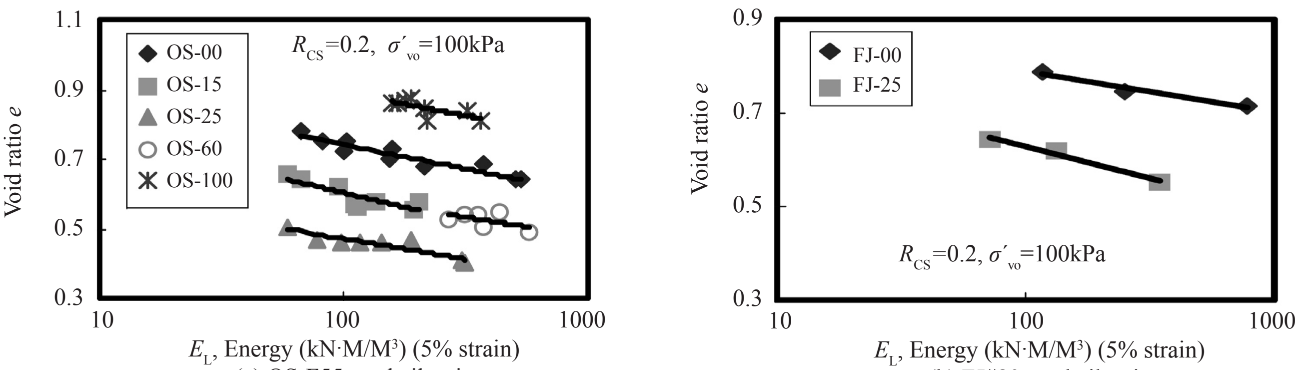

(a) OS-F55 sand-silt mix (b) FJ#80 sand-silt mix

Fig. 8 Energy to liquefaction – E_L vs. e

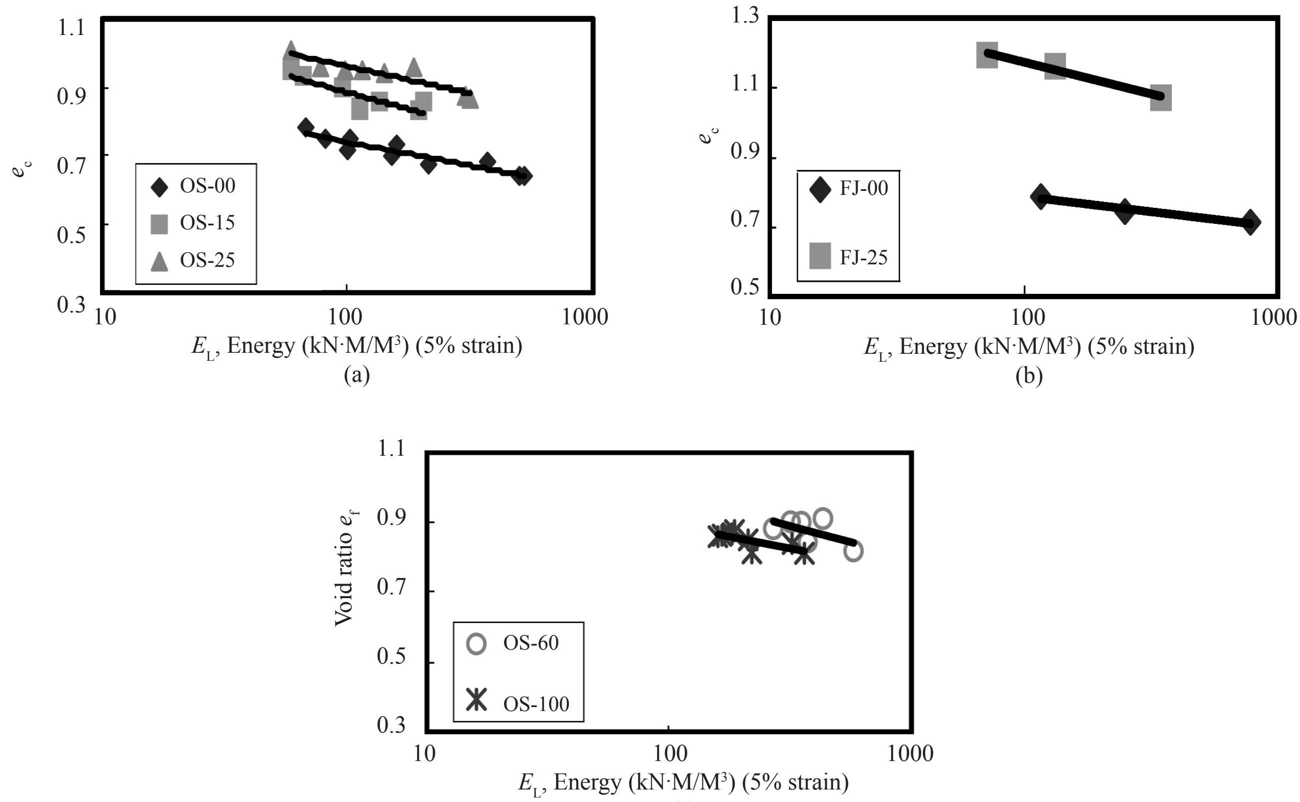

(a) (b) (c)

Fig. 9 E_L vs. e_c and e_f at R_{CS}=0.2

content up to C_{Fth} and then the void ratio required to resist liquefaction increases with further increase in silt content beyond C_{Fth}.

3.3.2 First-order Indices e_c and e_f

When the data for C_F<C_{Fth} is analyzed using e_c, silty sand requires more e*nergy to reach liquefaction than for the host sand at the same e_c (Figs.9(a) and (b). When the data for >*C_{Fth} is analyzed using e_f, sandy silt requires more energy to reach liquefaction than for the host silt at the same e_f (Fig.9(c)). The relationship between E_L and the first order-indices e_c and e_f are better than the relationship for E_L with global void ratio, but still no unique relationship is observed.

3.3.3 Second-order indices $(e_c)_{eq}$ and $(e_f)_{eq}$

The liquefaction resistance data is compared against $(e_c)_{eq}$ for C_F<C_{Fth} in Figs. 10 (a) and (b) and against $(e_f)_{eq}$ for C_F>C_{Fth} in Figs. 10 (c). The data for sand and silty sands fall in a narrow band in Fig.10 (a) for OS-F55 sand-silt mixes. Similar observation is made for FJ#80 in Fig.10 (b). Similarly, the data for sandy silt (C_F>C_{Fth}) merge with that of pure silt in Fig.10 (c).

These observations indicate the utility of the second-order contact density indices to study and characterize liquefaction resistance of granular mixes in a consistent manner.

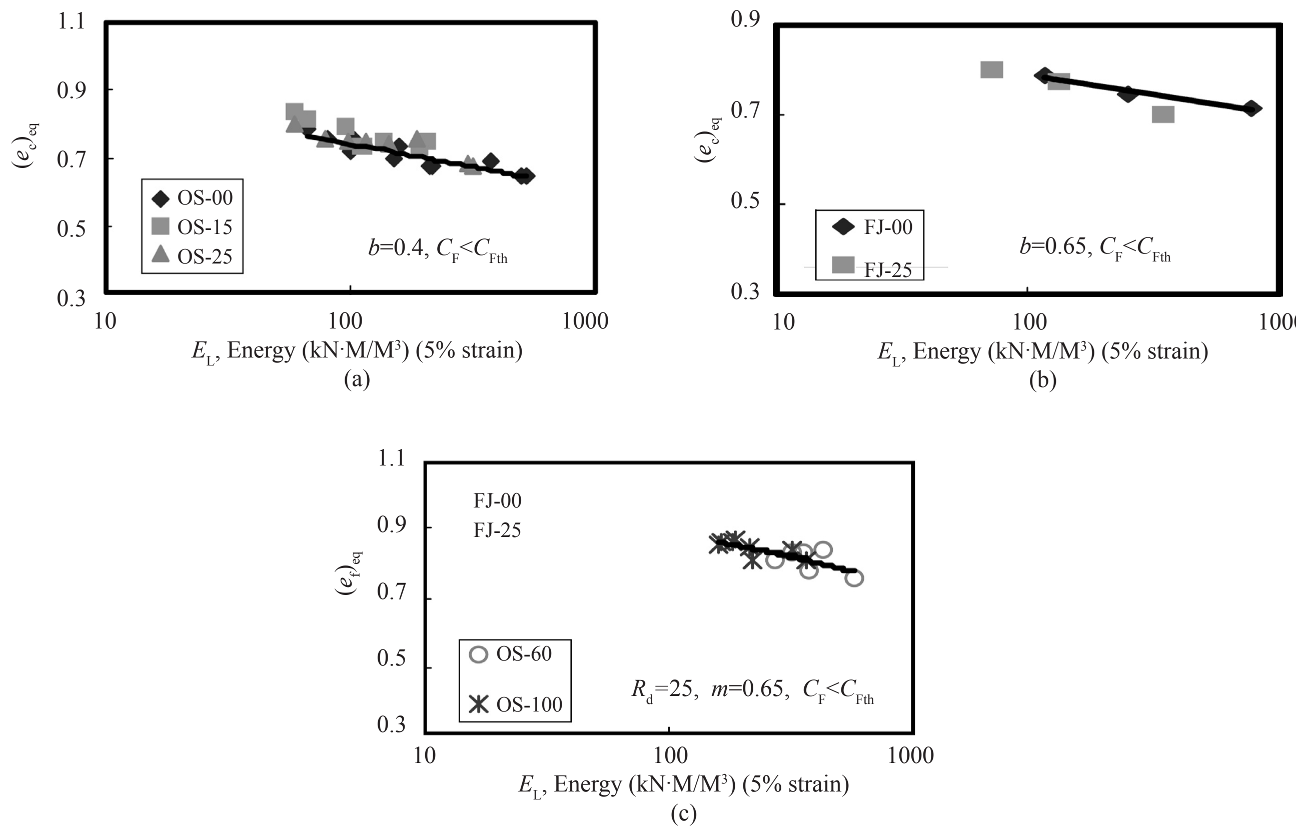

Fig. 10 E_L vs. $(e_c)_{eq}$ and $(e_f)_{eq}$ at R_{CS}=0.2

3.4 Liquefaction resistance of other soil mixes

The above framework was further evaluated using other available data on liquefaction resistance for other granular mixes in the published literature. Two examples are shown next by reinterpreting the data reported by Polito and Martin (2001). The data reported in Polito and Martin (2001) involved two sands, Monterey No. 0/30 sand (d_{50}=0.43mm) and Yatesville sand (d_{50}=0.18mm), each mixed with a non-plastic silt (Yatesville silt, d_{50}=0.03 mm) at silt contents ranging from 0 to 100% by weight and subjected to undrained cyclic triaxial tests on isotropic consolidated specimens. Figs.11 (a) and (b) show the original raw data, e versus cyclic stress ratio (CSR) R_{CS} required to cause liquefaction in 15 cycles for Monterey sand-silt and Yatesville sand-silt mixes, respectively. There is no unique relationship between R_{CS} and global void ratio for either soil mix.

3.4.1 Second-order indices $(e_c)_{eq}$ and $(e_f)_{eq}$

Reinterpreting these data using the framework presented in this paper, Figs. 12 (a) and (b) show the e_{min}, e_{max}, and transition zones for C_{Fth} and C_{FL} for Monterey sand-silt and Yatesville sand-silt mixes, respectively. The R_{CS} data are plotted against $(e_c)_{eq}$ for C_F<C_{Fth} and $(e_f)_{eq}$ for C_F>C_{Fth} in Figs.13 (a) and (b), respectively, for Monterey sand-silt mix and in Figs. 14 (a) and (b), respectively, for

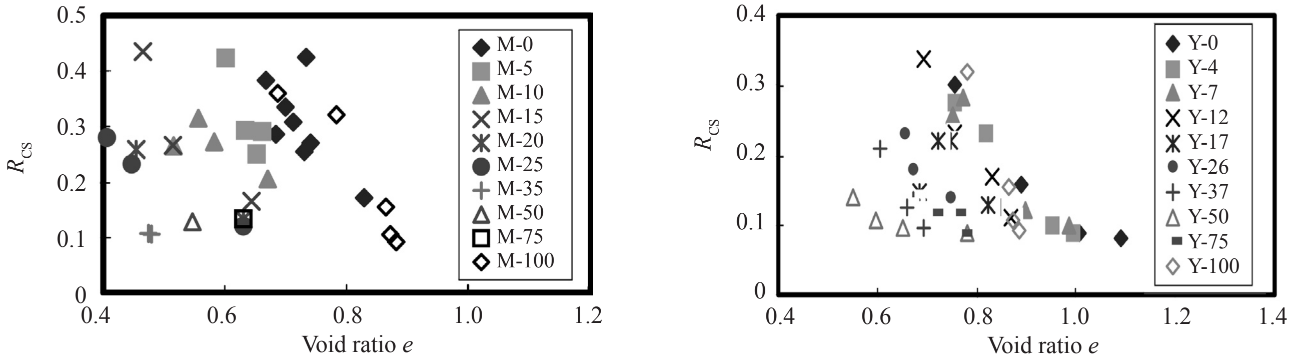

(a) Monterey sand-silt mix (b) Yatesville sand-silt mix

Fig. 11 Cyclic stress ratio at 15 cycles to liquefaction (M-20=Monterey sand with 20% silt, after Polito and Martin, 2001)

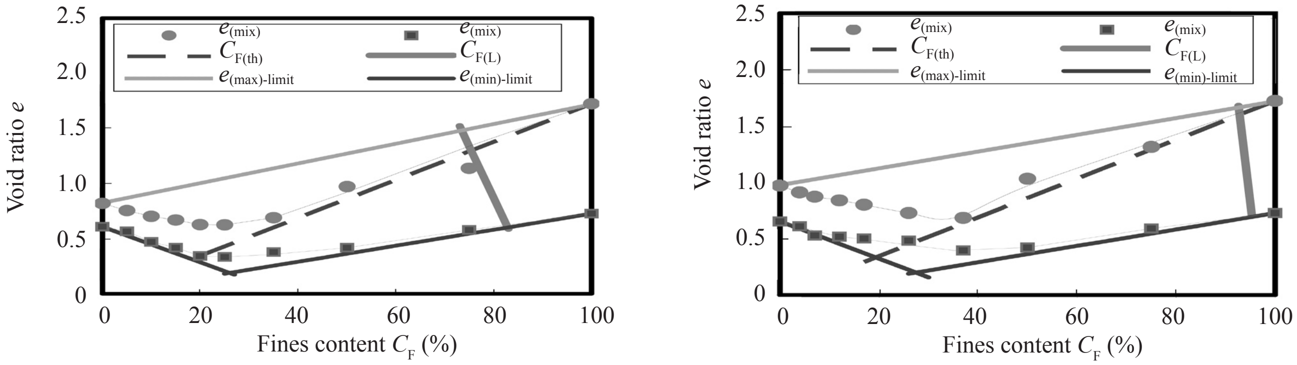

(a) Monterey sand-silt mix (b) Yatesville sand-silt mix

Fig. 12 e_{min}, e_{max}, C_{Fth} and C_{FL} Diagram

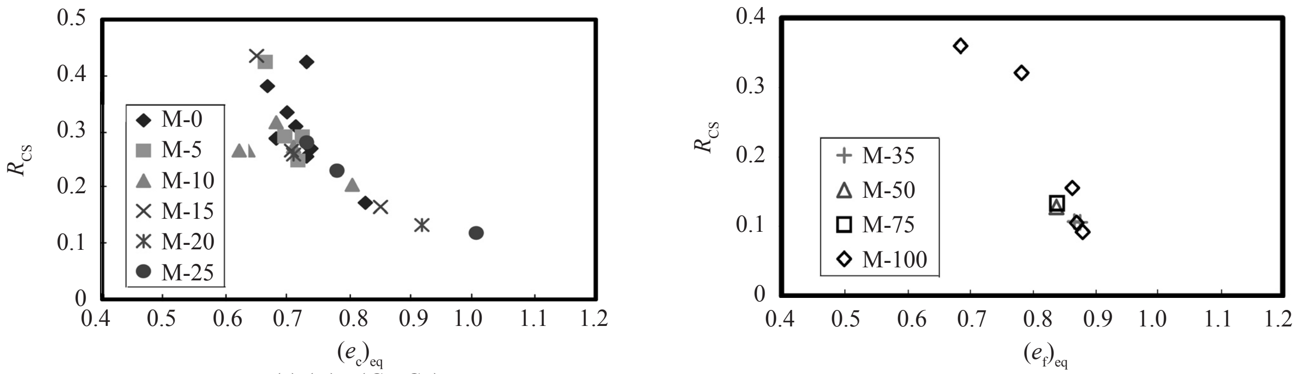

(a) $(e_c)_{eq}$ (C_F<C_{Fh}) (b) $(e_f)_{eq}$ (C_F>C_{Fth})

Fig. 13 C_{SR} versus contact index void ratios - Monterey sand-silt mix

Yatesville sand-silt mix. The R_{CS} data for both sand-silt mixes at C_F greater than the respective C_{Fth} are plotted against $(e_f)_{eq}$ in Fig.15. The parameters b and m are (0.25, 0.45) and (0.6, 0.6), respectively, for Monterey and Yatesville soil mixes, respectively (Kanagalingam and Thevanayagam, 2006).

The same observations found for the OS-F55 and FJ#80 sand silt mixes are also found for these two soil mixes as well. There exists a good correlation between R_{CS} and $(e_c)_{eq}$ for each soil mix at silt contents less than the threshold C_{Fth} values for each soil mix. Similarly, there is also a good correlation between and $(e_f)_{eq}$ for sandy silts for both soil mixes. These observations provide further support for the proposed framework.

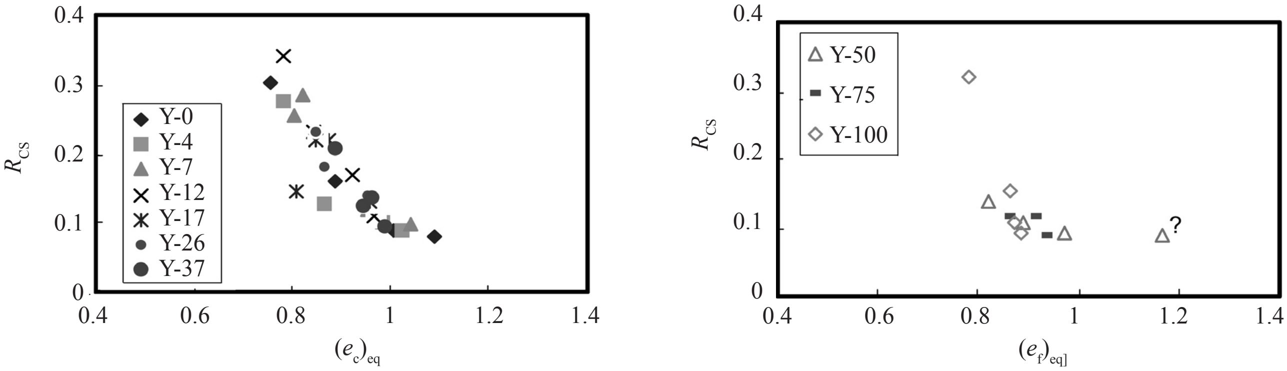

(a) $(e_c)_{eq}$ (C_F<C_{Fth}) (b) $(e_f)_{eq}$ (C_F>C_{Fth})

Fig. 14 C_{SR} versus contact index void ratios - Yatesville sand-silt mix

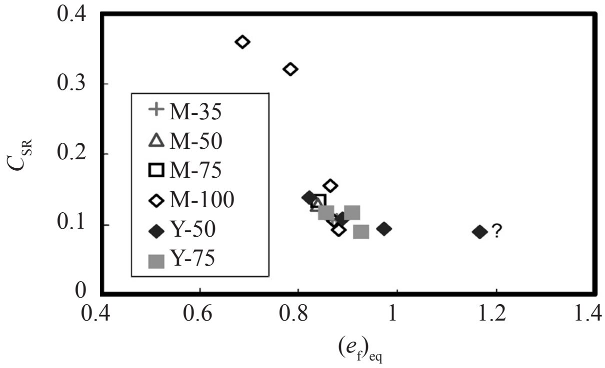

Fig. 15 R_{CS} versus $(e_f)_{eq}$ - Monterey sandy silt and Yatesville sandy silt at C_F>C_{Fth}

4 Conclusions

A simple framework for analysis of the relative effects of intergrain contacts on liquefaction resistance of granular mixes is presented. A set of first-order and second-order intergrain contact density indices (e_c, e_f), and (($e_c)_{eq}$, $(e_f)_{eq}$)), respectively, are introduced as possible indices for characterizing of the liquefaction resistance of granular mixes. Based on this framework and analyses of a limited amount of experimental data, the following observations are made.

(a) When compared at the same global void ratio e, the liquefaction resistance of a granular mix decreases with an increase in fine grains content up to a certain threshold value C_{Fth}. Beyond that, the liquefaction potential increases as the silt content increases. C_{Fth} depends on the grain characteristics of the host sand and fines, size disparity ratio, and the global void ratio.

(b) At low C_F (<C_{Fth}), when compared at the same e_c, an increase in fine grains content leads to a reduction in liquefaction resistance. Liquefaction resistance of a silty sand is similar to the host sand when compared at the same equivalent intergranular void ratio $(e_c)_{eq}$. The $(e_c)_{eq}$ is a useful index to characterize the liquefaction resistance of granular mixes at low silt contents.

(c) At high C_F (>C_{Fth}), when compared at the same e_f, an increase in finer grains content leads to an increase in liquefaction resistance. When compared at the same $(e_f)_{eq}$, the cyclic strength of a sandy silt is similar to that of the host silt. The $(e_f)_{eq}$ is a useful index to characterize liquefaction resistance of sandy silts.

Acknowledgements

Financial support for this research by the National Science Foundation and USGS/NEHRP program is gratefully appreciated. This research also benefited from other research conducted at University at Buffalo on liquefaction mitigation sponsored by MCEER and FHWA.

References

Andrews DCA (1998), "Liquefaction of Silty Soils: Susceptibility, Deformation, and Remediation," *PhD Dissertation*, Dept. of Civil Eng., CA, USC.

Andrews DCA and Martin GR. (2000), "Criteria for Liquefaction of Silty Soils," *Proc. 12th WCEE 2000 Conf.*, Auckland, NZ.

Berrill JB and Davis RO (1985), "Energy Dissipation and Seismic Liquefaction in Sands: Revised Model," *Soils and Found.*, Tokyo, **25**(2): 106-118.

Chameau JL and Sutterer K (1994), "Influence of Fines in Liquefaction Potential and Steady State Considerations," *Proc., 13th Intl. Conf. On Soil Mech. and Found. Eng.*, New Delhi, India, 183-84.

Chang NY (1990), "Influence of Fines Content and Plasticity on Earthquake-induced Soil Liquefaction," C*ontract No. DACW3988-C-0078*, US Army WES, MS.

Davis RO and Berrill, JB (1982), "Energy Dissipation and Seismic Liquefaction in Sands,," *Earthquake Engrg. and Struct. Dyn.*, **19**: 59-68

Davis RO and Berrill JB (1998a), "Energy Dissipation and Liquefaction at Port Island, Kobe," *Bull. New Zealand Nat. Soc. For Earthq. Engrg*., Waikanae, New Zealand, **31**: 31-50

Davis RO and Berrill JB (1998b), "Site-specific Prediction of Liquefaction," *Geotechnique*, London, **48**(2): 289-293

Desai CS (2000), "Evaluation of Liquefaction Using Disturbed State and Energy Approaches," *J. Geotech. & Geoenv. Eng.*, ASCE, **126**(7), 618-631

Evans MD and Zhou S (1995), "Liquefaction Behavior of Sand-gravel Composites," *J. Geoech. Eng*., ASCE, **121**(3): 287-298

Figueroa JL, Saada AS, Liang L and Dahisaria MN (1994), "Evaluation of Soil Liquefaction by Energy Principles," *J. Geotech. Engrg*., ASCE, **120**(9): 1554-1569.

Finn LWD, Ledbetter RH and Guoxi Wu (1994), "Liquefaction in Silty Soils: Design and Analysis," *ASCE Geotech. Spec. Publ.* 44, eds. S. Prakash and P. Dakoulas, 51-76.

Georgiannou VN, Burland JB and Hight DW (1990), "The Undrained Behaviour of Clayey Sands in Triaxial Compression and Extension," *Geotechnique*, **40**(3): 431-449.

Georgiannou VN Hight DW and Burland JB (1991), "Undrained Behaviour of Natural and Model Clayey Sands," *Soils and Foundations*, **31**(3): 17-29.

Ishihara K. (1993), "Liquefaction and Flow Failure During Earthquakes," *Geotechnique*, **43**(3): 351-41

JGS (1996),"Soils and Foundations - Special Issue on Geotechnical Aspects of the January 17, 1995 Hyogoken-Nambu Earthquake," *Japanese Soc. Geotech. Eng*.

Kanagalingam T (2006), Liquefaction Resistance of Granular Mixes Based on Contact Density and Energy Considerations," *PhD Dissertation*, University at Buffalo, SUNY, Buffalo, NY.

Kanagalingam T and Thevanayagam S (2006), "Contribution of Fines to the Compressive Strength of Mixed Soils," Discussion, *Geotechnique*.

Kayen RE and Mitchell JK (1997),"Assessment of Liquefaction Potnetialduring Earthquakes by Arias Intensity," *J. Geotech. And Geoenviron. Engrg*., ASCE, **123**(12): 1162-1174.

Koester JP (1994), "The Influence of Fines Type and Conent on Cyclic Strength," *Proc. ASCE Conv., Atlanta, Geotech.* Spec. Pub., 44: pp.17-32.

Kuerbis R, Nagussey D and Vaid YP (1988), "Effect of Gradation and Fines Content on the Undrained Response of Sand", *Proc. Conf. Hyd. Fill Struc*., ASCE Geot. Spec. Publ. 21: pp. 30-45

Law KT, Cao YL, and He GN (1990), "An Energy Approach for Assessing Seismic Liquefaction Potential," *Can. Geotech. J.,* Ottawa, **27**: pp.320-329.

Liang., L, Figueroa JL and Saada AS (1995), "Liquefaction Under Random Loading: Unit Energy Approach," *J. Geotech. Engrg.*, ASCE, **121**(11): 776-781.

Mitchell JK (1993), *Fundamentals of Soil Behavior,* 2nd Ed., John Wiley & Sons, Inc., New York, N.Y.

Nemat-Nasser S and Shokooh A (1979), "A Unified Approach to Densification and Liquefaction of Cohesionless Sand in Cyclic Shearing," *Can. Geotech. J.*, **16**: 659-678.

Ni Q, Tan TS, Dasari GR and Hight DW (2004), "Contribution of Fines to the Compressive Strength of Mixed Soils," *Geotechnique*, **54**(9): 561-569.

Pitman TD, Robertson PK and Sego DC (1994), "Influence of Fines on the Collapse of Loose Sands," *Can. Geotech. J.*, **31**: 728-739.

Polito CP and Martin II, JR (2001), "Effects of Nonplastic Fines on the Liquefaction Resistance of Sands," *J. Geotech. and Geoenv. Engrg.* Div., ASCE, **127**(5): 408-415.

Roscoe KH (1970), "The Influence of Strains in Soil Mechanics," *Geotechnique*, **20**(2): 129-170.

Seed HB (1987), "Design Problems in Soil Liquefaction", *J. Geot.. Eng. Div.* , ASCE, **113**(8): 827-45.

Seed RB and Harder LF Jr. (1990), "SPT-based Analysis of Cyclic Pore Pressure Generation and Undrained Residual Strength," *Proc., Seed Mem. Symp.*, **2:** pp. 351-376.

Seed HB, Idriss IM and Arango I (1983), "Evaluation of Liquefaction Potential Using Field Performance Data," *J. Geot.. Eng. Div.*, ASCE, **109**(3): 458-482.

Singh, S (1994), "Liquefaction Characteristics of Silts," *Ground Failures Under Seismic Conditions*, *Proc., ASCE Nat. Convention, Geotech Spec. Publ.* 44, S. Prakash and P. Dakoulas, eds., ASCE, Reston, Va., pp. 105-116.

Thevanayagam S (1998), "Effect of Fines and Confining Stress on Undrained Shear Strength of Silty Sands," *J. Geotech. & Geoenv. Engrg. Div.,* ASCE, **124**(6): 479-491.

Thevanayagam S (2000), "Liquefaction Potential and Undrained Fragility of Silty Sands," *Proc. 12th International Conf. Earthquake Engineering*, Auckland, New Zealand, eds. R. Park, paper #.2383.

Thevanayagam S (2007), "Intergrain Contact Density Indices for Granular Mixes – I: Framework," *J. Earthquake Engineering and Engineering Vibrations*, **6**(2).

Thevanayagam S, Ravishankar K and Mohan S (1996), "Steady State Strength, Relative Density and Fines Content Relationship for Sands," *TRB 1547*, pp. 61-67.

Thevanayagam S, Shenthan T and Kanagalingam T

(2003), “Role of Intergranular Contacts on Mechanisms Causing Liquefaction & Slope Failures in Silty Sands,” *Research Report*, http://erp-web.er.usgs.gov/reports/abstract/2001/pt/01hqgr0032-report.pdf, U.S. Geological Survey, Dept. of Interior, USA, 396p.

Thevanayagam S, Shenthan T, Mohan S and Liang J (2002), “Undrained Fragility of Sands, Silty Sands and Silt,” *J. Geotech. & Geoenv. Eng*., ASCE, **128**(10): 849-859.

Todorovska MI and Trifunac MD (1999), “Liquefaction Opportunity Mapping via Seismic Wave Energy,” *J. Geotech. & Geoenv. Engrg. Div*., ASCE, **125**(12): 1032-1042.

Trifunac MD (1995), “Empirical Criteria for Liquefaction in Sands via Standard Penetration Tests and Seismic Wave Energy,” *J. Soil Dyn. and Earthq. Eng.*, **14**: 419-426.

Vaid YP (1994), “Liquefaction of Silty Soils,” *ASCE Conv., Geotech. Spec. Publ*. 44: pp. 1-16.

Yamamuro JA and Lade PV (1998), “Steady-state Concepts and Static Liquefaction of Silty Sands,” *J. Geotech. and Geoenv. Engrg. Div.*, ASCE, **124**(9): 868-877.

Zlatovic S and Ishihara K (1997), “Normalized Behavior of Very Loose Non-plastic Soils: Effects of Fabric,” *Soils and Foundations,* **37**(4): 47-56.

Notations

The following symbols are used in this paper:

b = contribution factor representing influence of fine grains, $0<b<1$

R_{CS} = cyclic stress ratio

e = global void ratio

e_c = intergranular void ratio

e_f = interfine void ratio

$(e_c)_{eq}$ = equivalent intergranular void ratio

$(e_f)_{eq}$ = equivalent interfine void ratio

e_{max} = maximum void ratio

e_{min} = minimum void ratio

$e_{max,HC}$ = maximum void ratio of host coarse grain soil

$e_{min,HC}$ = minimum void ratio of host coarse grain soil

$e_{max,HF}$ = maximum void ratio of host fine grain soil

$e_{min,HF}$ = minimum void ratio of host fine grain soil

E_L = the required dissipated energy per unit volume of soil to reach liquefaction

C_F = percentage fines content

c_f = $FC/100$

C_{Fth} = threshold fines content

C_{FL} = limiting fines content

N_L = the number of cycles required to reach liquefaction

R_d = size disparity ratio (D/d)

σ'_{vo} = initial effective confining stress

τ = shear stress

γ = shear strain

m = reinforcement factor